DOI 10.1007/s11106-018-9952-6
Powder Metallurgy and Metal Ceramics, Vol. 57, Nos. 1-2, May, 2018 (Russian Original Vol. 57, Nos. 1-2, Jan.-Feb., 2018)

KINETICS OF NONISOTHERMAL PRESSURE SINTERING OF ZIRCONIUM DIBORIDE POWDER WITH ADDITIVES OF BORON AND CHROMIUM CARBIDES IN VACUUM

V. B. Vinokurov,[1] M. S. Kovalchenko,[1,2] L. I. Klimenko,[1] N. D. Bega,[1] and T. V. Mosina[1]

UDC 621.(762.5+77):66-982+669.(296+781)

The analysis of the experimental data on the kinetics of nonisothermal pressure sintering of zirconium diboride-based powder mixtures with the addition of boron and chromium carbides in vacuum showed a division of the sintering temperature mode into low-temperature and high-temperature areas. The division is clearly observed when the temperature increases at a rate of 20°C/min. In low-temperature area, the densification occurs slowly and hardly depends on the temperature. In high-temperature area, the viscous flow of the matrix of the porous material is controlled by the power-law creep of the matrix forming the porous body with an activation energy of 394 kJ/mol. Twofold increase in heating rate leads to acceleration of low- and high-temperature strain of the matrix and increase in the apparent activation energy to 581 kJ/mol, indicating the series engagement of additional mechanisms of material flow. The investigation of structure and properties of materials has showed that the formation of new boron–carbide phases and eutectic that disappears during sintering activates the densification of the porous material. It is found out that under low pressure nonisothermal sintering, a superplasticity phenomenon can occur, which results in the densification of the porous body to the virtually non-porous state.

Keywords*: zirconium diboride, boron and chromium carbides, pressure sintering in vacuum, densification kinetics, structure, properties.*

INTRODUCTION

In 1956, Department for Refractory Compounds headed by Grigorii V. Samsonov has been established at the Institute of Metal Ceramics and Special Alloys of the Academy of Sciences of the UkrSSR (the Institute for Problems of Materials Science of the Academy of Sciences of the UkrSSR since 1964). The basic scientific direction of this Department was the synthesis of metal-like and non-metal refractory compounds (carbides, nitrides, borides, silicides, sulfides, phosphides, arsenides), the study of their crystal structure, chemical, physical, and mechanical properties of these compounds to create hard high-temperature materials for various purposes on their basis. Based on the personal experience, Samsonov knew that the synthesis of majority of refractory compounds should be carried out at temperatures significantly lower than their melting temperature and, as a result, obtained these compounds in powder form [1]. This was also confirmed by the experience in synthesizing tungsten

[1]Frantsevich Institute for Problems of Materials Science, National Academy of Sciences of Ukraine, Kyiv, Ukraine.

[2]To whom correspondence should be addressed; e-mail: mskoval@ipms.kiev.ua.

Translated from Poroshkova Metallurgiya, Vol. 57, Nos. 1–2 (519), pp. 35–49, 2018. Original article submitted January 15, 2018.

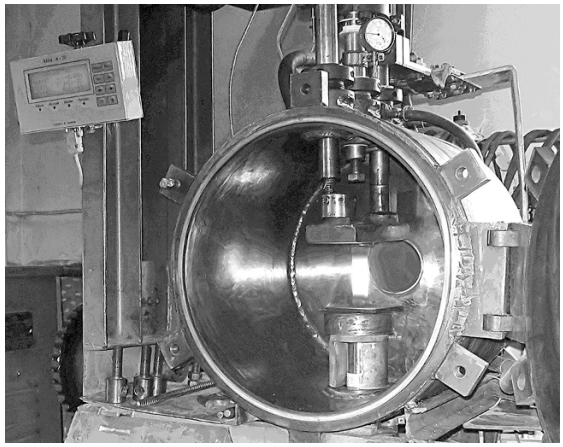

Fig. 1. Laboratory installation for vacuum pressure sintering of powder materials

carbide in producing hardmetals. Therefore, further processing of powders must be carried out exclusively by powder metallurgy methods. The only acceptable method for producing low-porosity samples to study their physical and mechanical properties was pressure sintering or hot pressing, combining pressing and sintering in one process. Samsonov acquired his experience in pressure sintering of powders during his postgraduate studies, when he was assigned to produce high-density boron carbide disks as absorber elements for developing nuclear reactors. This knowledge has been used for manufacturing of hot-pressing laboratory press in the pilot plant of the Institute of Metal Ceramics and Special Alloys. Actually, that is when the systematic study of pressure sintering of powders of refractory compounds has begun [2–13].

In the late 1960s, the accumulated experience in hot pressing was used for designing and producing high-temperature laboratory vacuum press. As a result, Design Bureau of the Institute has produced compact, simple, and easy-maintenance installation that, after modernizing and fitting with modern means of control, has allowed to explore the behavior of refractory materials at high temperatures. Vacuum in 0.05 m^3 chamber is created by two mechanical pumps and diffusion unit. Heating of graphite dies is ensured by direct transmission of low-voltage (<8 V) electric current supplied from the mains through power and adjusting standard transformers, and AC regulator. The shrinkage is recorded using a dilatometric device. The loading of the press rod with up to 5000 N using compound lever ensures the maintenance of strictly fixed pressure, which is hardly achievable in hydraulic presses. When high-strength graphite is used as die material, the installation allows obtaining up to 14 mm dia. samples. When using 8 mm dia. dies, sintering can be performed under pressure up to 100 MPa at temperatures up to 2500°C with controlled heating rate ranging from 1 to 1500°C/min. Figure 1 shows the appearance of the press vacuum chamber.

The above installation parameters allow investigating the regularities of pressure sintering, the formation of structure and properties of ceramic composite materials based on refractory compounds used in thermal power engineering, aerospace, and other fields of modern technics. Among this class of materials, zirconium diboride based composites are of special interest [14–20]. These composites demonstrate sufficient strength at higher temperatures, compared to other similar materials.

At the same time, past and current researches in some cases are focused on searching the additives activating sintering of composites and not reducing their strength properties, when operating. Higher chromium carbide can be used as an effective activating additive. The positive effect of using Cr_3C_2 is due to fact that, in the presence of refractory borides [20] and nitrides [21], lower chromium carbides are formed and atomic carbon is released, which is used for removing oxygen from the system and is a part of the new refractory compounds. This enables obtaining high-temperature ceramics with lower energy costs. However, the use of chromium borides and carbides as sintering activators leads to formation of plastic interlayers between ZrB_2 grains that reduce high-temperature strength and creep temperature of the composites.

The purpose of this study is to investigate the densification kinetics of zirconium diboride powder mixture with additives of chromium and boron carbides during the nonisothermal pressure sintering in vacuum and the structure and some properties of the sintered material.

MATERIALS AND EXPERIMENTAL PROCEDURE

The study was carried out using the powders of zirconium diboride ZrB_2 and chromium carbide Cr_3C_2 made by JSC Donetsk Plant of Chemical Reagents (Table 1).

Grinding and mixing of powders were conducted in a caprolon-lined ball mill. As grinding media, we used tungsten carbide-based standard hardmetal balls and hot-pressed boron carbide balls. During grinding, due to wear of boron carbide grinding media, fine-dispersed boron carbide powder was added to the mixture; the amount of the added powder was controlled subject to the wear of balls. The grinding of ZrB_2 and Cr_3C_2 powder mixture using B_4C grinding media for 100 and 150 h resulted in mean particle size of 2 and 0.9 μm, respectively. The time preparation of mixtures using hardmetal balls lasted 24 h.

The sintering temperature and the change in the sample height were controlled using an infrared thermometer Thermix K and linear displacement transducer, respectively. The current values of temperature and linear shrinkage of the sample were recorded automatically every 5 sec. Based on the values of the current linear shrinkage x_i, of the final relative density ρ_f and height h_f of the samples, the current values of the relative density were determined according to the formula [13]:

$$\rho = \frac{\gamma_f h_f}{(h_0 - x_i)\gamma_{th}}, \quad (1)$$

where $h_0 = h_f + x_f$ is the initial height; γ_{th} is the theoretical density.

The particle-size distribution of powders and mixtures was determined using a SK Laser Micron Sizer laser analyzer. The phase composition of the samples was X-ray analyzed in CuK_α-radiation with nickel filter using a DRON-4 diffractometer in a digital scanning mode. The powder LaB_6 was used as an external reference. Diffraction patterns were processed using software for initial processing (New-profile, Rayflex) and PDF-2 database. Metallographic studies were performed using a MIM-10 optical microscope. The hardness was measured using a Falkon 509 device (Netherlands) under indentation load 200 N.

Due to small size of the samples, the mechanical properties of the material (fracture toughness K_{Ic}, contact tensile σ_f and compression Y strength, and microstructure strength of ceramics S_{ms}) were assessed by indentation at room temperature according to the procedures [22–24].

DENSIFICATION KINETICS OF POWDER MIXTURE DURING NONISOTHERMAL PRESSURE SINTERING

The study of densification kinetics of powder materials enables choosing rational processing modes for obtaining materials with the required service properties, given the data about the formation of their structure and properties. Experimental studies of pressure sintering are performed using the starting powder ZrB_2 and mixtures with the volume content of the components, %: 91.5 ZrB_2 + 8.5 B_4C (mixture 1); 82.4 ZrB_2 + 17.6 B_4C (mixture 2); 80 ZrB_2 + 2 Cr_3C_2 + 18 B_4C (mixture 3).

TABLE 1. Chemical Composition and Mean Size d of Particles for Starting Powders

Compound	Mass content of doping elements, %						d, μm
	O_2	C_{total}	C_{free}	Fe	B	B_2O_3	
ZrB_2	1.10	0.03	–	0.10	18.80	0.30	7.70
Cr_3C_2	1.10	12.70	0.10	0.11	–	–	9.10

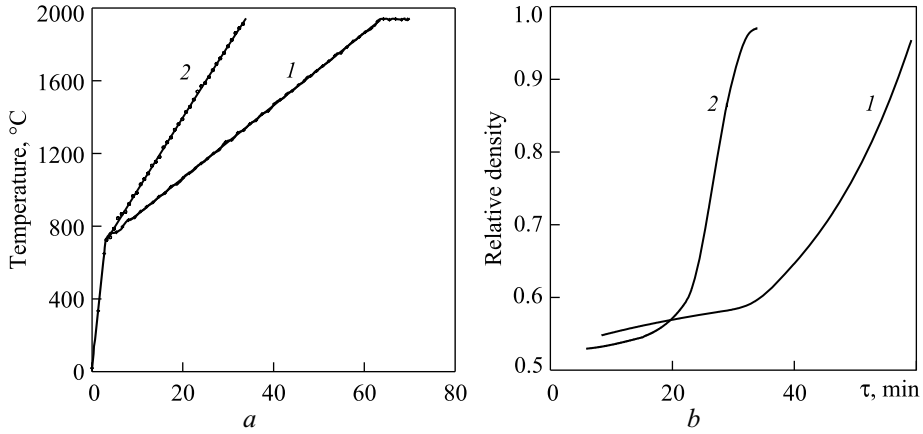

Fig. 2. Variation of temperature (*a*) and relative density (*b*) of powder mixture with 80 vol.% ZrB_2 + 2 vol.% Cr_3C_2 + 18 vol.% B_4C during nonisothermal sintering under 48 MPa and heating rate 20 (*1*) and 39°C/min (*2*) with sintering time

The experimental pressure sintering of the starting powder ZrB_2 under 48 MPa with rapid (within 2 min) heating up to 2150°C and isothermal holding up to 30 min showed the damped shrinkage in time and the achievement of the relative density $\rho = 0.9$. In similar rapid heating and isothermal holding at 2150°C, the ground mixtures 1 and 2 are sintered under the same pressure with the achievement of the relative density $\rho = 0.929$ and $\rho = 0.947$, respectively. In similar heating mode up to 1940°C, the ground mixture 3 is sintered under the same pressure with the achievement of the relative density $\rho = 0.981$. These data indicate that B_4C and Cr_3C_2 additives activate sintering of zirconium diboride and densification of mixture 3 during pressure sintering requires more detailed study. Therefore, nonisothermal sintering of the mixture with the variation of heating rate and applied pressure has been studied. Due to some scattering, the resulting data on the variation of temperature and relative density with sintering time were subject to piecewise polynomial least-squares fit [25]. Cubic polynomials were used. Figure 2 shows smoothed data about the effect of heating rate on the appearance of compacting curves under pressure.

Densification kinetics of the porous viscous body is described by the equation that expresses the relative decrease in its volume V and associated density in time t under the effect of Laplacian pressure P_L generated by the surface tension of the material in the pores and external axial pressure P:

$$-\frac{1}{V}\frac{dV}{dt} = \frac{1}{\rho}\frac{d\rho}{dt} = -\frac{1}{1-\theta}\frac{d\theta}{dt} = \frac{P_L}{\zeta} + \frac{P}{Z}, \tag{2}$$

where ρ is the relative density; $\theta = 1 - \rho$ is the porosity; ζ is the volume viscosity during uniform bulk compression; and Z is the volume viscosity during body compression in a cylindrical die [26]. The values ζ and Z are determined by the equations:

$$\zeta = \frac{1}{3}\eta_0 \frac{2+\rho^{2/\rho}}{1-\rho^{2/\rho}}\rho^{(2.5-\rho)/\rho}; \tag{3}$$

$$Z = \eta_0 \frac{2-\rho^{2/\rho}}{1-\rho^{2/\rho}}\rho^{(2.5-\rho)/\rho}, \tag{4}$$

where η_0 is the dynamic shear viscosity of the matrix forming the porous body. The values Z and ζ are related by the ratio:

$$Z = \frac{3\zeta}{1+2\xi}, \tag{5}$$

where ξ is the coefficient of lateral pressure (when pressed in the die) equals to $\xi = \nu/(1 - \nu)$ (here ν is the coefficient of lateral strain: in the theory of elasticiny it is the Poisson ratio). For incompressible viscous body $\nu = 0.5$ and, when approaching to a non-porous state, $\xi \to 1$ and $Z \to \zeta$. Therefore, when $P > P_L$, the pressure implies the sum $P + P_L$.

The resulting ratios for the volume viscosity describe the viscous behavior of Newtonian porous viscous body, whose shear flow rate $\dot{\varepsilon}$ of the matrix linearly depends on the shear stress τ. The viscous flow of crystalline materials, as proven by numerous experiments based on their steady-state creep at high temperatures, obeys the nonlinear power law

$$\dot{\varepsilon} = \frac{1}{2} A \left(\frac{\tau}{\tau_0} \right)^n , \tag{6}$$

where τ_0 is the threshold stress of material shear; n is the power exponent of non-linearity for viscous flow ($n > 1$);

$$A = \text{ const } \frac{D_0 \mu_m b}{k_B T} \exp \left(-\frac{U}{k_B T} \right) , \tag{7}$$

D_0 is the pre-exponential factor for the volume self-diffusion coefficient; U is the activation energy; μ_m is the shear modulus; k_B is the Boltzmann constant [27]. After conversion of Eq. (2), we obtain the equation of densification kinetics of the porous body under pressure, controlled by the power-law steady-state creep mechanism at high temperatures close to melting temperatures [26]:

$$\frac{d}{dt} X_d (n, \rho) = \rho^{(n-3)/2} \psi^{(n+1)/2} \frac{d\rho}{dt} = \frac{AP^n}{2\tau_0^n} , \tag{8}$$

where $X_d (n, \rho)$ is the integral function of density,

$$X_d (n, \rho) = \int_{\rho_0}^{\rho} \rho^{(n-3)/2} \psi^{(n+1)/2} d\rho = \int_{\rho_0}^{\rho} \rho^{\frac{2.5(n+1)-4\rho}{2\rho}} \left(\frac{2 - \rho^{2/\rho}}{2\left(1 - \rho^{2/\rho}\right)} \right)^{(n+1)/2} d\rho; \tag{9}$$

$$\psi = \frac{2 - \rho^{2/\rho}}{2(1 - \rho^{2/\rho})} \rho^{(2.5-\rho)/\rho} . \tag{10}$$

The substitution of (7) into (8) and taking the logarithm provide a linear dependence of the logarithm of rate change in the relative density change on the reciprocal temperature T^{-1}:

$$\ln \left(T \frac{d}{dt} X_d (n, \rho) \Big/ \left(\frac{P}{\tau_0} \right)^n \right) = \text{ const } - \frac{U}{k_B T} , \tag{11}$$

which can be used for assessing the activation energy of the matrix creep forming the porous body. Evaluating the activation energy during the pressure sintering of powders allows one to neglect the decrease in the threshold stress τ_0 of the matrix, which occurs at higher temperatures. Then, the logarithm determines by the product of three values: temperature T, equation $\rho^{(n-3)/2} \psi^{(n+1)/2}$, and densification rate $\dot{\rho} = (d/dt)\rho$.

Figure 3 shows (by points, with an interval of 4 numerical values) the curves calculation of $\ln \left(T (d/dt) X_d (n, \rho) \right)$ versus the reciprocal thermodynamic temperature T^{-1} during pressure sintering of mixture 3 carried out with integer values of the flow non-linearity exponent n from 1 to 5 and $n = 4.5$ for heating rates $(d/dt)T$ equal to 20 and ~39°C/min.

Figure 3*a* shows the inflection on the curves of the logarithms $\ln \left(T (d/dt) X_d (n, \rho) \right)$ versus the reciprocal temperature T^{-1} that divides high- and low-temperature sintering areas of the material studied. It is also observed in Fig. 3*b*; however, it is pronounced less sharply and at higher temperature. In high-temperature area,

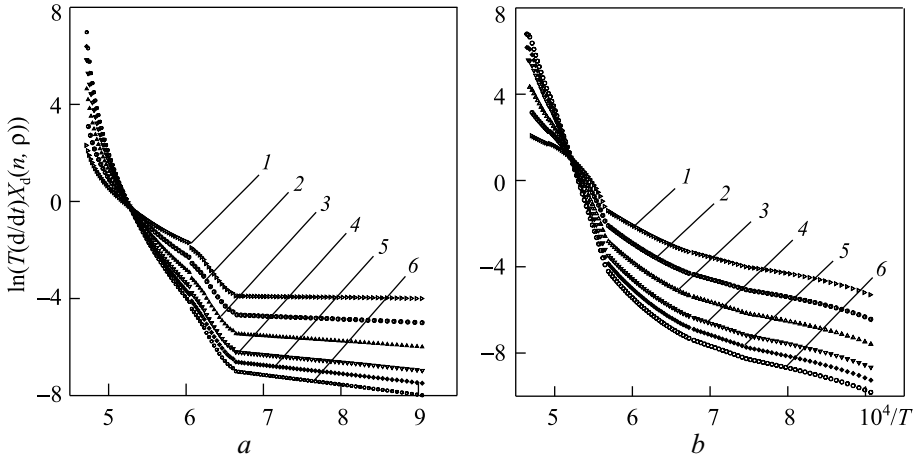

Fig. 3. Calculated curves of $\ln\left(T\left(\mathrm{d}/\mathrm{d}t\right)\mathrm{X_d}\left(n,\,\rho\right)\right)$ versus reciprocal thermodynamic temperature T^{-1} with flow non-linearity exponent n, equal to 1 (*1*), 2 (*2*), 3 (*3*), 4 (*4*), 4.5 (*5*), and 5 (*6*), for sintering powder mixture 3 under 48 MPa with heating rate 20 (*a*) and 39°C/min (*b*)

when the values of the non-linearity index of viscous flow of the matrix forming the porous body are ≥4, the logarithms of compacting function rates are linear in relation to the reciprocal temperature and comply with the theory of volume viscous flow controlled by the power-law creep of polycrystalline materials. This is also confirmed by the activation energy value, determined according to the linearity of the logarithm $\ln\left(T\left(\mathrm{d}/\mathrm{d}t\right)\mathrm{X_d}\left(n=4{,}5,\,\rho\right)\right)$ versus the reciprocal temperature T^{-1} for heating rate 20°C/min (Fig. 3*a*), equal to 394 kJ/mol. Low-temperature area (Fig. 3*a*) can be attributed to the plastic strain of the matrix forming the porous body. If high-temperature areas for selected heating rates are in general similar, then, low-temperature areas differ in both the slope of the logarithm with respect to the reciprocal temperature axis and pronounced curvature of this dependence. This enables concluding that increasing heating rate includes mechanisms of activated sliding of dislocations, for which the activation energy decreases as the root mean square stresses in the matrix of the porous body increase [28]. This is indicated by pronounced non-linear behavior of dependencies in low-temperature area (Fig. 3*b*).

Despite the external similarity of the curves (Fig. 3), the transition from low-temperature into high-temperature area with higher heating rate (Fig. 3*b*) is shifted towards higher temperatures; furthermore, the slope of the lines with respect to the reciprocal temperature axis in high-temperature area is bigger than in Fig. 3*a*. Consequently, the activation energy value turns out to be considerably higher than 394 kJ/mol and makes 581 kJ/mol for the slope of the line $\ln\left(T\left(\mathrm{d}/\mathrm{d}t\right)\mathrm{X_d}\left(n=4,\,\rho\right)\right)$. This divergence in the activation energy values can be explained by the fact that two-fold increase in heating rate to the non-linear mechanism initiates the series engagement of additional mechanisms increasing the overall strain rate at the same shear stress [29, 30].

We can observe (Figs. 3*a* and 3*b*) that the calculated curves of $\ln\left(T\left(\mathrm{d}/\mathrm{d}t\right)\mathrm{X_d}\left(n,\,\rho\right)\right)$ versus the reciprocal temperature T^{-1} with different values n intersect in one point. Different temperatures (1623 and 1648°C) and virtually the same relative density (0.7382 and 0.7388) correspond to these points, respectively (Figs. 3*a* and 3*b*). Ignoring Laplacian pressure, the root mean square stress $\langle\tau\rangle = P/\sqrt{\rho\psi}$ in this point under P = 48 MPa is assessed to be 71.7 MPa. The assessed value is too high to indicate the transition from power-law non-linear creep to linear diffusion one. During sintering of metals and refractory compounds in isothermal pressure sintering, the nonlinear creep controls the compacting while achieving the relative density >0.9, and in some cases >0.95 [1, 7–13, 26].

Figure 3*a* shows that, at the final sintering stage, the curves of $\ln\left(T\left(\mathrm{d}/\mathrm{d}t\right)\mathrm{X_d}\left(n,\,\rho\right)\right)$ versus the reciprocal temperature T^{-1} reveal an ascendant curvilinear trend. This can be explained by features of heating the

die with sample by direct pass of electric current. At the initial and intermediate sintering stages, heating is due to heat release in graphite die; the sintering temperature being determined by the temperature of the die surface. With compacting conductive sample, its electrical resistance decreases to the values lower than those of electrical resistance of graphite and heat release of the sample exceeds that of its die that leads to increase in the temperature gradient from its center to the surface. This reason causes errors in determining the temperature of the sample. Therefore, the above ascendant curvilinear trend of the curves is associated with effect of principle heat release in the sample at the final sintering stage.

The study of sintering mixture 3 with rapid temperature increase and subsequent isothermal holding at 1940°C with and with no external pressure with changing its fixed values from 6 to 48 MPa has revealed a lack of regular achievement of the final density value from pressure. Depending on the applied pressure, the relative density values are sequenced as follows:

Pressure, MPa	0	6	12	24	36	48
Relative density	0.961	0.996	0.952	0. 898	0.925	0.981

High relative density of the sample, sintered with no external pressure indicates fairly high Laplacian pressure generated by surface tension in the powder of micron and submicron particle sizes. This pressure is roughly estimated to be 10–15 MPa. This Laplacian pressure is much higher than the external axial pressure and the sintering conditions approach those of bulk compression. Under these conditions, the lateral shrinkage reduces the diameter of the sample. The decrease in the diameter of the sample from 8 to 5.6 mm was experimentally recorded.

Being abnormal at first glance, the relative density obtained by sintering powder mixtures under the external pressure only 6 MPa is due to structural superplasticity [31] of the matrix of the porous body. To maintain the superplastic flow, certain conditions should be fulfilled. First of all, it is a grain fineness of the starting structure of the material (<2 μm) and a constant energy dissipation rate in the system. Another essential condition is the simultaneous action of two flow mechanisms of the material: non-linear mechanism providing uniform flow and accommodation mechanism adjusting the structure in such a way that the material maintains integrity and grain fineness. The non-linearity of superplastic flow n is from 2 to 3. The superplasticity can be implemented only during pressure sintering through a programmable pressure increase, while at constant pressure by programmable increase in the temperature that the viscosity of the matrix forming the porous body exponentially depends upon. The nonisothermal sintering of mixture 3 under 6 MPa induced favorable conditions that enabled the superplasticity. It could not appear under higher pressures, because of the high starting strain rate of the matrix under the action of the high root-mean-square stresses.

STRUCTURE AND PROPERTIES OF SINTERED MATERIALS

X-ray analysis of the phase composition of sintered zirconium diboride based composite samples allows discussing the changes in their phase composition during sintering. Fragments of X-ray patterns of the samples are presented below true to scale, as the reflections of activating additives are at the background level.

During pressure sintering of the starting ZrB_2 powder at 2150°C, a small amount of ZrC (which is due to use of graphite tooling) and ZrB_{12} phase are formed (Fig. 4*a*). Along with ZrB_2, the samples of mixture 1 with 8.5% B_4C sintered at 1940°C contain ZrC, B_4C, and boron and zirconium oxides in small amounts. The increase in the sintering temperature up to 2150°C and simultaneous increase of B_4C content up to 17.6 vol.% in mixture 2 hardly change the phase composition of the samples (Fig. 4*b*).

Significant changes in the phase formation of mixture 3 with 2 vol.% Cr_3C_2 are observed. Already at the beginning of sintering at 1550°C, the decomposition of Cr_3C_2 into lower carbides and the formation of $Cr_{23}C_6$ phase are reported. Also, the phases ZrB_2, B_4C, ZrC, ZrO_2, and B_2O_3 are present (Fig. 5*a*). During nonisothermal sintering with heating rate 20°C/min up to 1940°C, in addition to the main components, we detected a gradual decomposition of higher chromium carbide into the phases: $Cr_3C_2 \rightarrow Cr_7C_3 \rightarrow Cr_{23}C_6$ with release of free carbon (Fig. 5*b*). This confirms that the decomposition of Cr_3C_2 into lower carbides with the formation of Cr–$Cr_{23}C_6$ eutectic activates ZrB_2 densification.

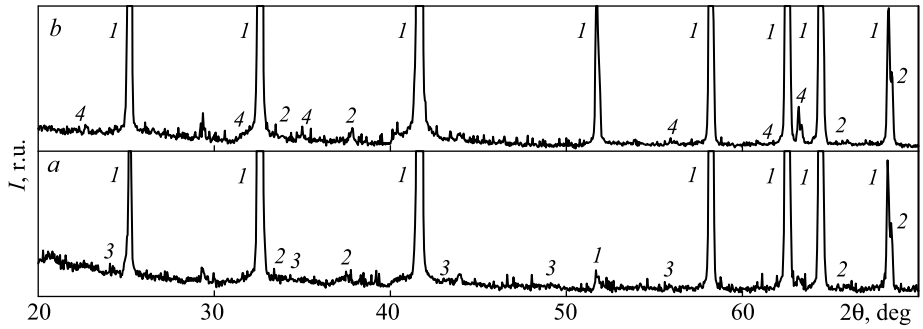

Fig. 4. Fragments of X-ray patterns of samples sintered under 48 MPa at 2150°C from starting powder ZrB_2 (*a*) and mixture 2 with volume content 82.4% ZrB_2 + 17.6% B_4C (*b*). Lines of identified phases: ZrB_2 (*1*); ZrC (*2*); ZrB_{12} (*3*); B_4C (*4*)

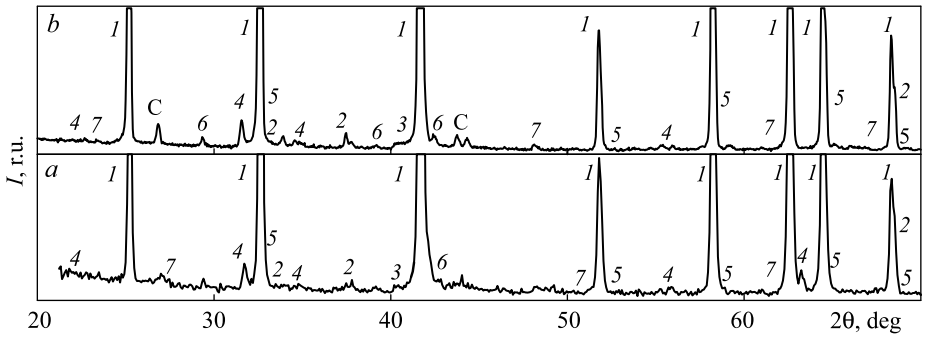

Fig. 5. Fragments of X-ray patterns of samples sintered under 48 MPa from mixture 3 with volume content 80% ZrB_2 + 2% Cr_3C_2 + 18% B_4C at 1550 (*a*) and 1940°C (*b*) with heating rate 20°C/min. Lines of identified phases: ZrB_2 (*1*); ZrC (*2*); ZrB_{12} (*3*); B_4C (*4*); Cr_3C_2 (*5*); Cr_7C_3 (*6*); $Cr_{23}C_6$ (*7*); carbon (C)

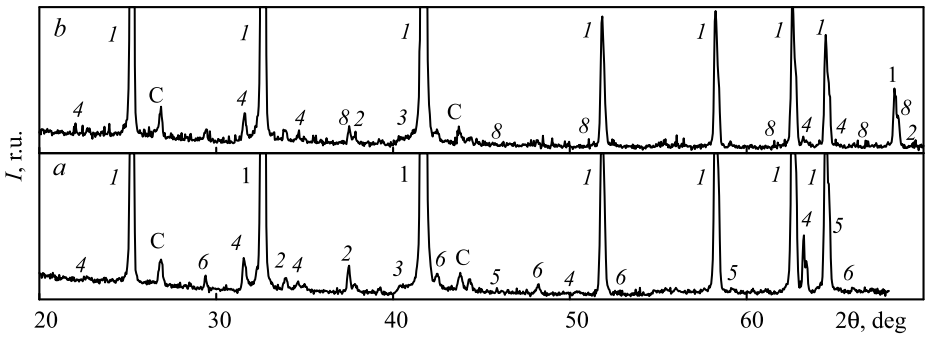

Fig. 6. Fragments of X-ray patterns of samples sintered at 1940°C from mixture 3 with volume content 80% ZrB_2 + 2% Cr_3C_2 + 18% B_4C under 6 (*a*) and 24 MPa (*b*). Lines of identified phases: ZrB_2 (*1*); ZrC (*2*); ZrB_{12} (*3*); B_4C (*4*); Cr_3C_2 (*5*); Cr_7C_3 (*6*); Cr_5B_3 (*8*); carbon (C)

Figure 6 shows the fragments of X-ray patterns of samples of mixture 3 sintered under 6 and 24 MPa. The phase composition of the sample with the relative density $\rho = 0.996$, sintered under 6 MPa, contains chromium carbides (Fig. 6*a*). In addition to the main components, the composition of the sample with the relative density $\rho = 0.898$ sintered under 24 MPa contains refractory Cr_5B_3 (Fig. 6*b*).

Figure 7 shows structures and hardness indentations on the sample surface. The samples of pure zirconium diboride have relatively low hardness equal to 10.42 GPa; thin and long cracks occur during testing. The hardness of zirconium diboride with B_4C additives decreases to 9.98 GPa, leaf-shaped cracks occur during testing, and the

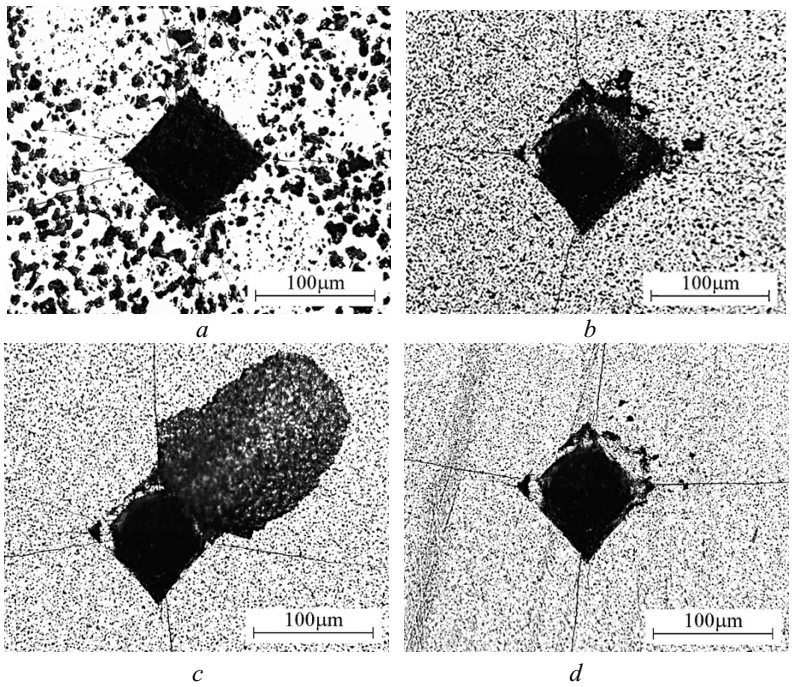

Fig. 7. Appearance of hardness indentations on surface of samples sintered of starting powder ZrB_2 (*a*) and ZrB_2 powder mixtures with volume content of additives 8.5% B_4C (*b*), 17.6% B_4C (*c*), and 2% Cr_3C_2 + 18% B_4C (*d*)

TABLE 2. Properties of ZrB_2-Based Composite Samples Sintered at 1940°C under 48 MPa

Composition, vol.%	ρ	HV_{2N}, GPa	HV_{200N}, GPa	$K_{Ic\ 200}$, MPa · $m^{1/2}$	$\sigma_{f\ 200}$, GPa	*Y*, GPa	S_{ms}, GPa
Starting* ZrB_2	0.900	15.25	10.42	4.91	0.36	1.33	0.50
ZrB_2 + 17.6 B_4C	0.930	11.60	9.98	7.06	0.58	1.12	1.18
ZrB_2 + 2 Cr_3C_2 + 18 B_4C	0.981	15.64	12.64	4.32	0.35	1.79	0.43
	0.967	11.63	13.26	4.32	0.35	1.95	0.43

* Sintering temperature 2150°C.

material breaks off. Mixture 3 sintered samples containing B_4C and Cr_3C_2 additives possess higher hardness ranging from 11.8 to 13.3 GPa.

Table 2 displays some mechanical properties of the material: hardness *HV* under 2 and 200 N load, fracture toughness K_{Ic}, contact strength in tension σ_f and compression *Y*, and microstructure hardness of ceramics at room temperature S_{ms}.

CONCLUSIONS

Nonisothermal pressure sintering of powder zirconium diboride-based mixtures with additions of boron and chromium carbides in vacuum, structurization and properties of the sintered material have been experimentally studied. It has been established that the introduction of stated additives leads to occurrence of new boron–carbide phases and eutectic disappearing when sintering. They activate the densification and enable achieving high density, formation of heterophase structure enhancing the mechanical properties of the material at room and high temperatures.

The quantitative analysis of compacting kinetics of zirconium diboride powder mixture with additives of boron and chromium carbides in nonisothermal sintering under constant pressure and various heating rate using experimental data from the volume viscous flow position has demonstrated the division of the temperature mode into low- and high-temperature areas. Such division is more pronounced, when heating rate 20°C/min.

In low-temperature area, the densification occurs slowly and hardly depends on the temperature. In high-temperature area, the viscous matrix flow of the porous material is controlled by the power-law creep of the matrix forming the porous body with activation energy of 394 kJ/mol.

Two-fold increase in heating rate leads to acceleration in low- and high-temperature strain of the matrix and increase in the apparent activation energy up to 581 kJ/mol, indicating the series engagement of additional mechanisms of material flow. It has been found out that, in low-temperature area, the increase in heating rate leads to development of thermally activated plastic strain with low activation energy depending on mechanical stresses acting in the material.

At the final sintering stage below the threshold value of the root-mean-square stress, the power-law creep of the matrix forming the porous body transforms into the linear diffusion creep.

Abnormal densification of the powder mixture containing additives of boron and chromium carbides up to the relative density 0.996 in nonisothermal sintering under 6 MPa has been identified. Such density has proved to be unachievable, when sintering under pressures exceeding 6 MPa by a factor of 2–6. The abnormal behavior of the mixture when sintering can be explained by the superplasticity phenomenon induced by the effect of two flow mechanisms, when the constant rate of dissipation energy is kept.

REFERENCES

1. M. S. Kovalchenko, “Hot pressing of powders of refractory compounds and materials based on them,” *Powder Metall. Met. Ceram.*, **37**, Nos. 1–2, 37–44 (1998).
2. G. V. Samsonov and M. S. Kovalchenko, “Some aspects of sintering refractory compound,” *Powder Metall. Met. Ceram.*, No. 1, 20–29 (1961).
3. G. V. Samsonov and M. S. Kovalchenko, “Application of viscous flow theory in sintering of powders of refractory compounds by hot pressing,” *Powder Metall. Met. Ceram.*, No. 2, 3–13 (1961).
4. M. S. Kovalchenko and G. V. Samsonov, “Viscous flow during sintering of zirconium boride by hot pressing,” *Powder Metall. Met. Ceram.*, No. 5, 3–9 (1961).
5. G. V. Samsonov and M. S. Kovalchenko, *Hot Pressing* [in Russian], Gostekhizdat UkrSSR, Kyiv, (1962), p. 212.
6. M. S. Kovalchenko and Yu. I. Rogovoi, “Microstructure of hot-pressed molybdenum carbide,” *Powder Metall. Met. Ceram.*, **9**, No. 12, 1013–1017 (1970).
7. M. S. Kovalchenko and L. F. Ochkas, “Creep in the hot pressing of titanium carbide powder,” *Powder Metall. Met. Ceram.*, **12**, No. 1, 23–31 (1973).
8. M. S. Kovalchenko, “Creep in the hot pressing of powders of titanium nitride, molybdenum disilicide, zirconium and chromium diborides,” *Powder Metall. Met. Ceram.*, **12**, No. 4, 272–276 (1973).
9. M. S. Kovalchenko and M. M. Mai, “Creep in the hot pressing of titanium diboride powder,” *Powder Metall. Met. Ceram.*, No. **12**, 8, 622–225 (1973).
10. M. S. Kovalchenko and L. F. Ochkas, “Creep in the hot pressing of Zirconium carbide powder,” in: *3-d All-Union Scientific-Technical Conference on Metal–Ceramic Materials and Products* [in Russia], Izdat. Yerevan Politekh. Inst., Yerevan (1973), pp. 139–143.
11. M. S. Kovalchenko, “Creep in hot pressing of powders of some refractory compounds,” in: *Sintering: Theory and Practice*, ed. by M. M. Ristic, Herceg-Novi (1973), p. 308–316.
12. M. S. Kovalchenko, *Fundamentals of Heat Treatment of Porous Materials by Pressure* [in Russian], Nauk. Dumka, Kiev (1980), p. 238.
13. M. S. Kovalchenko, “Pressure sintering kinetics of tungsten and titanium carbides,” *Int. J. Ref. Met. Hard Mat.*, **39**, 32–37 (2013).

14. F. Monteverde, D. D. Fabbriche, and Bellosi," Zirconium diboride-based composites," *Key Eng. Mater.*, **206–213**, 961–964 (2002).
15. J. J. Meléndez-Martínez, A. Domínguez-Rodriguez, F. Monteverde, et al., "Characterisation and high temperature mechanical properties of zirconium boride-based materials," *J. Europ. Ceram. Soc.*, **22**, Nos. 14–15, 2543–2549 (2002).
16. A. L. Chamberlain, W. G. Fahrenholtz, and G. E. Hilmas, "Low-temperature densification of zirconium diboride ceramics by reactive hot pressing," *J. Am. Ceram. Soc.*, **89**, No. 12, 3638–3645 (2006).
17. J. K. Sonber, T. S. R. Ch. Murthy, C. Subramanian, et al., "Investigations on synthesis of ZrB_2 and development of new composites with HfB_2 and $TiSi_2$," *Int. J. Ref. Met. Hard Mat.*, **29**, 21–30 (2011).
18. Eric W. Neuman, "Elevated temperature mechanical properties of zirconium diboride based ceramics," (2014). Doctoral Dissertations. 2164. Path to the source http://scholarsmine.mst.edu/doctoral_dissertations/2164.
19. M. W. Bird, R. P. Aune, A. F. Thomas, et al., "Temperature-dependent mechanical and long crack behavior of zirconium diboride–silicon carbide composite," *J. Europ. Ceram. Soc.*, **32**, 3453–3462 (2012).
20. O. N. Grigiriev, V. B. Vinokurov, L. I. Klimenko, et al., "Sintering of zirconium doboride and phase transformations in the presence of Cr_3C_2," *Powder Metall. Met. Ceram.*, **55**, Nos. 3–4, 185–194 (2016).
21. V. G. Kayuk and V. A. Maslyuk, "Structure formation in alloys of the Cr_3C_2–TiN system and the properties of materials based on them," *Powder Metall. Met. Ceram.*, **43**, Nos. 1–2, 39–43 (2004).
22. B. A. Galanov and O. N. Grigoriev, "Analytical model for indenting brittle materials," in: *Electronic Microscopy and Strength of Materials*. Frantsevich Institute for Problems of Materials Science, NAS Ukraine, Issue 13, Kiev (2006), pp. 4–42.
23. B. A. Galanov, O. N. Grigoriev, and E. G. Trunova, "Static Characteristics of Contact Strength of Ceramics," in: *Electronic Microscopy and Strength of Materials*, Frantsevich Institute for Problems of Materials Science, NAS Ukraine, Issue 8, Kiev (2001), pp. 125–135.
24. O. N. Grigoriev, B. A. Galanov, V. A. Kotenko, et al., "Contact strength and fracture toughness of brittle materials," *Metallofiz. Nov. Tekhnol.*, No. 8, 1001–1018 (2005).
25. A. Ango, *Mathematics for Electrical and Radio Engineers* [Russian translation], Nauka, Moscow (1965), p. 779.
26. M. S. Kovalchenko, "Pressure sintering of powder materials," *Powder Metall. Met. Ceram.*, **50**, Nos. 1–2, 18–33 (2011).
27. D. S. Wilkinson and M. F. Ashby, "Pressure sintering by power law creep," *Acta Met.*, **23**, No. 11, 1277–1285 (1975).
28. V. V. Skorokhod, *Rheological Bases of Sintering Theory* [in Russian], Nauk. Dumka, Kiev (1972), p. 152.
29. M. S. Kovalchenko, "Joint effects of various flow mechanisms in a porous polycrystalline body in hot pressing. Part I. General theory," *Powder Metall. Met. Ceram.*, **30**, No. 7, 562–566 (1991).
30. M. S. Kovalchenko, "Combined effect of different flow mechanisms of a porous crystalline body in hot compacting. Part III. Successive connection model," *Powder Metall. Met. Ceram.*, **30**, No. 9, 730–734 (1991).
31. M. V. Grabsky, *Structural Superplasticity of Metals* [Russian translation], Metallurgizdat, Moscow (1975), p. 269.